

Johnson Matthey Highlights

A selection of recent publications by Johnson Matthey R&D staff and collaborators

Brazing Filler Metals

M. Way, J. Willingham and R. Goodall, *Int. Mater. Rev.*, 2020, **65**, (5), 257

Brazing is a joining technique that is more than 5000 years old. It is a versatile technique that is still fundamental to some of the biggest engineering challenges faced today. The ability to join dissimilar material combinations (for example, metal-ceramic joints) is one of the unique advantages it has over other joining methods. With widespread interest in brazing with filler metal development for many future technologies, this review discusses practice and theory of brazing and advanced filler metal development, progress and opportunities.

Long- and Short-Range Magnetism in the Frustrated Double Perovskite Ba_2MnWO_6

H. Mutch, O. Mustonen, H. C. Walker, P. J. Baker, G. B. G. Stenning, F. C. Coomer and E. J. Cussen, *Phys. Rev. Mater.*, 2020, **4**, (1), 014408

Using neutron powder diffraction, DC magnetometry, muon spin relaxation and INS, the magnetic and structural properties of the fcc double perovskite Ba_2MnWO_6 were investigated. At a Néel temperature of 8(1) K with a frustration index, $f \approx 8$, Ba_2MnWO_6 undergoes type II long-range antiferromagnetic ordering. The magnetic coupling constants J_1 and J_2 , were found to equal -0.080 meV and -0.076 meV, respectively. They were identified by using INS. This indicated that both of the magnetic coupling constants are antiferromagnetic with similar magnitudes, in contrast to other known 3d metal double perovskites of the form Ba_2MWO_6 . Similarly to that observed in the archetypical fcc lattice antiferromagnet manganese oxide, above the Néel temperature, INS techniques and muon spin-relaxation measurements identify a short-range correlated magnetic state.

Improved Ambient Stability of Thermally Annealed Zinc Nitride Thin Films

A. Trapalis, I. Farrer, K. Kennedy, A. Kean, J. Sharman and J. Heffernan, *AIP Adv.*, 2020, **10**, (3), 035018

The stability of zinc nitride with a three-order magnitude increase in degradation time from a few days in unannealed films to several years after annealing is reported in this article. It shows that post-growth thermal annealing significantly improves the stability. Using samples annealed under a flow of nitrogen at 200–400°C, a degradation study was carried out. It showed the stability of the films was strongly dependent on the annealing temperature. A mechanism for the improvement is proposed and the result has substantial potential for using zinc nitride in devices where the application requires operational stability.

Structures of Mixed Manganese Ruthenium Oxides $(\text{Mn}_{1-x}\text{Ru}_x)\text{O}_2$ Crystallised Under Acidic Hydrothermal Conditions

L. K. McLeod, G. H. Spikes, R. J. Kashtiban, M. Walker, A. V. Chadwick, J. D. B. Sharman and R. I. Walton, *Dalton Trans.*, 2020, **49**, (8), 2661

This work reports on the synthesis of the solid solution β -(Mn,Ru) O_2 . Previous reports of mixed manganese-ruthenium oxides do not provide compelling evidence for the formation of a genuine mixed oxide. A new synthesis method was used successfully to form a solid solution. The complete range of techniques, probing long- and short-range atomic order and surface composition and structure provided evidence for the formation of mixed oxides. The tetragonal lattice parameters do not change isotropically, consistent with the different local environments of the two cations even though powder XRD indicates an expansion of the unit cell volume on replacement of manganese by ruthenium in the

rutile structure. The local structure as determined by EXAFS supports this conclusion.

Synthesis and Polymorphism of Mixed Aluminum-Gallium Oxides

D. S. Cook, J. E. Hooper, D. M. Dawson, J. M. Fisher, D. Thompsett, S. E. Ashbrook and R. I. Walton, *Inorg. Chem.*, 2020, **59**, (6), 3805

An investigation into the synthesis of a new solid solution of the oxyhydroxide $\text{Ga}_{5-x}\text{Al}_x\text{O}_7(\text{OH})$ was conducted using solvothermal reaction between gallium acetylacetonate and aluminum isopropoxide in 1,4-butanediol at 240°C. A limited compositional range was produced showing a linear contraction in unit cell volume with an increase in aluminium content. This study and results provide reference data for understanding structure-property relationships in the gallium oxide polymorphs for applications including electronics and photocatalysis as well as the long-standing study of aluminium oxides as catalyst supports in heterogeneous catalysis.

Temperature Reversible Synergistic Formation of Cerium Oxyhydride and Au Hydride: A Combined XAS and XPDF Study

A. H. Clark, N. Acerbi, P. A. Chater, S. Hayama, P. Collier, T. I. Hyde and G. Sankar, *Phys. Chem. Chem. Phys.*, 2020, **22**, (34), 18882

This article provides evidence for the formation of a gold hydride species at elevated temperature. Using high energy resolved fluorescence detection XANES and X-ray total scattering, *in situ* studies on the physical and chemical properties of gold in inverse ceria alumina supported catalysts have been conducted between 295 K and 623 K. It is proposed, through modelling of total scattering data to extract the thermal properties of gold using Grüneisen theory of volumetric thermal expansion, that the gold hydride formation occurs synergistically with the formation of a cerium oxyhydride. In a reducing atmosphere, the temperature reversible nature of the reaction demonstrates the activation of hydrogen without consumption of oxygen from the ceria lattice.

Adsorbate-Induced Segregation of Cobalt from PtCo Nanoparticles: Modeling Au Doping and Core AuCo Alloying for the Improvement of Fuel Cell Cathode Catalysts

B. Farkaš, C. B. Perry, G. Jones and N. H. de Leeuw, *J. Phys. Chem. C*, 2020, **124**, (33), 18321

The critical factors affecting segregation in platinum-cobalt-gold ternary and platinum-cobalt binary nanoparticles in the presence of oxidising species were identified. This was achieved using first-principles-based theoretical methods. At low

oxygen concentrations, and with a decreasing share of platinum, surface segregation of cobalt atoms was already thermodynamically viable in the platinum-cobalt systems. Gold was introduced as a dopant, which resulted in structural changes favouring the segregation of cobalt. Calculations demonstrated that cobalt leakage would be significantly suppressed through the creation of a cobalt-gold alloy core, owing to modification of the electronic properties. The theoretical framework used in this study provides a new route for the design of oxygen reduction catalysts.

Elucidating the Mechanism of the CO₂ Methanation Reaction Over Ni-Fe Hydrotalcite-Derived Catalysts via Surface-Sensitive *in situ* XPS and NEXAFS

G. Giorgianni, C. Mebrahtu, M. E. Schuster, A. I. Large, G. Held, P. Ferrer, F. Venturini, D. Grinter, R. Palkovits, S. Perathoner, G. Centi, S. Abate and R. Arrigo, *Phys. Chem. Chem. Phys.*, 2020, **22**, (34), 18788

NEXAFS and *in situ* XPS techniques were implemented to study the chemical nature of hydrotalcite-derived nickel and iron-promoted hydrotalcite-derived nickel catalysts under reaction conditions. During the reaction, hydroxylation of the nickel surface was shown to follow the formation of water. Higher selectivity towards carbon monoxide was detected when nickel surface hydroxylation was increased. In contrast, a dominant metallic nickel surface was shown to have higher selectivity towards methane. When selectivity to methane was high, electronic structure analysis revealed the existence of mostly Fe(III) species at the surface and a combination of Fe(II) and Fe(III) species under the surface. Fe(II) was observed to have a beneficial effect on the maintenance of nickel in a metallic state. Extending iron oxidation has a negative impact on methane selectivity, through a more extended nickel surface hydroxylation.

Use of Open Source Monitoring Hardware to Improve the Production of MOFs: Using STA-16(Ni) as a Case Study

F. Massingberd-Mundy, S. Poulston, S. Bennett, H. H.-M. Yeung and T. Johnson, *Sci. Rep.*, 2020, **10**, 17355

Low-budget (< US\$100) *in situ* reaction monitoring was used to demonstrate the ability to improve the MOF synthesis route of STA-16(Ni) (**Figure 1**). In a step-up from previous research, this study demonstrated the production of the MOF at atmospheric pressure. After just one experiment, an improvement in reaction time was predicted, with a reduction of 93%. This time reduction will be of great benefit in both academia

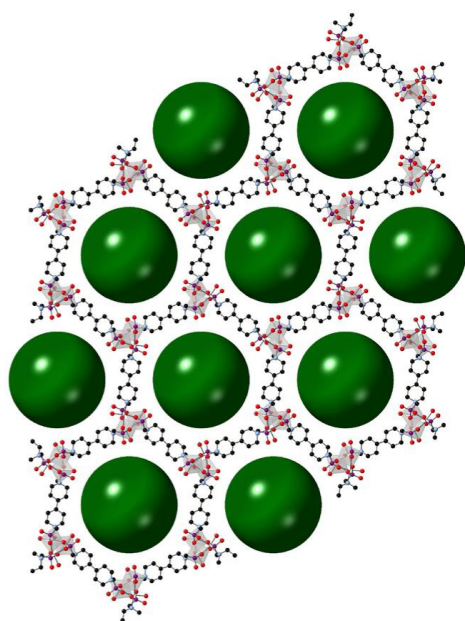


Fig. 1. Representation of the STA-16(Ni) framework. Black, light blue, red and purple spheres represent carbon, nitrogen, oxygen and phosphorous atoms respectively. Ni–O polyhedra are represented in light grey and green spheres ($r=2$ nm) are used to illustrate the pore voids. Protons omitted for clarity. Reprinted under Creative Commons Attribution 4.0 International (CC BY 4.0)

and industry, particularly with the minimal cost, low experimental overhead and few resources required.

Quantitative Carbon Distribution Analysis of Hydrocarbons, Alcohols and Carboxylic Acids in a Fischer-Tropsch Product from a Co/TiO₂ Catalyst During Gas Phase Pilot Plant Operation

R. Partington, J. Clarkson, J. Paterson, K. Sullivan and J. Wilson, *J. Anal. Sci. Technol.*, 2020, **11**, 42

Quantitative distribution analysis of oxygenated and FT hydrocarbon products was observed for a cobalt/titania catalyst used in a fixed bed gas phase pilot plant utilising CANSTM (Johnson Matthey, UK) catalyst carrier devices. This was achieved through a combination of methods, including GC-MS, GCxGC, GC and HPLC. The combination of techniques ensured a detailed exploration of the FT product composition. The average concentration of 1-alcohol, aldehyde, 1-olefin, *cis*- and *trans*-2-olefins were also quantified using ¹³C NMR and ¹H NMR analyses. As carbon chain

length increased, the 1-olefin:*n*-paraffin ratio in the hydrocarbon liquid and wax products was found to decrease significantly.

Establishing Reactivity Descriptors for Platinum Group Metal (PGM)-Free Fe–N–C Catalysts for PEM Fuel Cells

M. Primbs, Y. Sun, A. Roy, D. Malko, A. Mehmood, M.-T. Sougrati, P.-Y. Blanchard, G. Granozzi, T. Kosmala, G. Daniel, P. Atanassov, J. Sharman, C. Durante, A. Kucernak, D. Jones, F. Jaouen and P. Strasser, *Energy Environ. Sci.*, 2020, **13**, (8), 2480

Kinetic ORR activities, TOF and site-density (SD) values were analysed for four of the most active benchmark pgm-free iron/nitrogen doped carbon electrocatalysts using an *ex situ* gaseous carbon monoxide cryo chemisorption and an *in situ* electrochemical nitrate reduction. Rational catalyst developments were enabled through the utilisation of 'reactivity maps' as new analytical tools to deconvolute ORR reactivities. Substantial SD values paired with low TOF were observed for microporous catalysts, with the opposite noted for mesoporous catalysts. It is hoped that this research will help to improve pgm-free fuel cell cathode catalysts by acting as a reference for future knowledge-based research.

Palladium Dispersion Effects on Wet Methane Oxidation Kinetics

P. Velin, C.-R. Florén, M. Skoglundh, A. Raj, D. Thompsett, G. Smedler and P.-A. Carlsson, *Catal. Sci. Technol.*, 2020, **10**, (16), 5460

Palladium-alumina catalysts with systematically varied palladium oxide dispersions were prepared by incipient wetness impregnation. Controlled calcination was used to achieve a realistic contact between the alumina support and active palladium oxide nanoparticles. As the palladium oxide particle size increased in dry conditions, the apparent activation energy for methane oxidation also increased. It decreased in wet conditions. Active sites at the rim of the palladium oxide particles in contact with the alumina support were more sensitive to wet conditions than palladium oxide sites farther away from the rim, which can be attributed to more severe blocking by hydroxyl groups formed by water dissociation. In order to balance palladium utilisation and water tolerance in palladium–alumina catalysts for high methane TOF, palladium oxide particles should be ≥ 2 nm.